K* vector and tensor couplings from $N_f = 2$ twisted mass QCD

P. Dimopoulos,[1] F. Mescia,[2] and A. Vladikas[3]

(ETM Collaboration)

[1]*Dipartimento di Fisica, Università di Roma "Tor Vergata" Via della Ricerca Scientifica 1, I-00133 Rome, Italy*
[2]*Departament d'Estructura i Constituents de la Matéria and Institut de Ciéncies del Cosmos,*
Universitat de Barcelona, Diagonal 647, E-08028 Barcelona, Spain
[3]*INFN, Sezione di "Tor Vergata" c/o Dipartimento di Fisica,*
Università di Roma "Tor Vergata" Via della Ricerca Scientifica 1, I-00133 Rome, Italy

The mass m_{K^*} and vector coupling f_{K^*} of the K^* meson, as well as the ratio of the tensor to vector couplings $\frac{f_T}{f_V}|_{K^*}$, are computed in lattice QCD. Our simulations are performed in a partially quenched setup, with two dynamical (sea) Wilson quark flavors, having a maximally twisted mass term. Valence quarks are either of the standard or the Osterwalder-Seiler maximally twisted variety. Results obtained at three values of the lattice spacing are extrapolated to the continuum, giving $m_{K^*} = 981(33)$ MeV, $f_{K^*} = 240(18)$ MeV, and $\frac{f_T(2 \text{ GeV})}{f_V}|_{K^*} = 0.704(41)$.

I. BASICS

The aim of the present paper is to present novel lattice results for the mass of the K^* meson, as well as its vector and tensor couplings (f_V and f_T respectively), defined in Euclidean space-time as follows:

$$\langle 0|V_j|K^*; \lambda \rangle = -if_V \epsilon_j^\lambda m_{K^*}, \tag{1.1}$$

$$\langle 0|T_{0j}|K^*; \lambda \rangle = -if_T \epsilon_j^\lambda m_{K^*}. \tag{1.2}$$

In the above expressions, $V_j = \bar{s}\gamma_j d$ is the vector current (spatial components only; $j = 1, 2, 3$), $T_{0j} = i\bar{s}\sigma_{0j}d$ is the tensor bilinear operator (temporal component), and ϵ_j^λ denotes the polarization vector.

Our results are based on simulations of the ETM Collaboration (ETMC) [1], with $N_f = 2$ dynamical flavors (sea quarks) and "lightish" pseudoscalar meson masses in the range 280 MeV $< m_{PS} <$ 550 MeV. With three lattice spacings ($a = 0.065$ fm, 0.085 fm, and 0.1 fm) we are able to extrapolate our results to the continuum limit. Our simulations are performed with the tree-level Symanzik improved gauge action. For the quark fields we adopt a somewhat different regularization for sea and valence quarks. The sea quark lattice action is the so-called maximally twisted standard tmQCD (referred to as "standard tmQCD case") [2]. The $N_f = 2$ light sea quark flavors form a flavor doublet $\bar{\chi} = (\bar{u}, \bar{d})$ and the fermion lattice Lagrangian in the so-called "twisted basis" is given by

$$\mathcal{L}_{tm} = \bar{\chi}[D_W + i\mu_q \gamma_5 \tau^3]\chi, \tag{1.3}$$

where τ^3 is the isospin Pauli matrix and D_W denotes the critical Wilson-Dirac operator. By "critical" we mean that, besides the standard kinetic and Wilson terms, the operator

also includes a standard, nontwisted mass term, tuned at the critical value of the quark mass (κ_{cr} in the language of the hopping parameter), so as to ensure maximal twist. With only two light dynamical flavors, strangeness clearly enters the game in a partially quenched context.[1] For the valence quarks we use the so-called Osterwalder-Seiler variant of tmQCD, which consists in maximally twisted flavors which, unlike the standard tmQCD case, doublets:

$$\mathcal{L}_{OS} = \sum_{f=d,s} \bar{q}_f[D_W + i\mu_f \gamma_5]q_f, \tag{1.4}$$

with $\text{sign}(\mu_f) = \pm 1$ (see below for details). This action, introduced in Ref. [4] and implicitly used in [5], has been studied in detail in Ref. [6]. For the case in hand (i.e. K^*-related quantities) we only need down- and strange-quark flavors in the valence sector. Note that the choice of maximally twisted sea and valence quarks implies $\mathcal{O}(a)$ improvement of the physical quantities (i.e. the so-called automatic improvement of masses, correlation functions, and matrix elements) [7]. Thus unitarity violation, which plagues any partially quenched theory at finite lattice spacing, is an $\mathcal{O}(a^2)$ effect.

The sign of μ_s may be that of μ_d or its opposite. We conventionally refer to the setup in which $\text{sign}(\mu_d) = -\text{sign}(\mu_s)$ as the "standard twisted mass regularization" (denoted by tm) and the setup with $\text{sign}(\mu_d) = \text{sign}(\mu_s)$ as the "Osterwalder-Seiler regularization" (OS). Quenched pseudoscalar masses and decay constants in tm and OS setups have already been studied [8,9]. Having at our disposal two lattice regularizations in the valence quark

---

[1]In partially quenched lattice QCD, some flavors (e.g. strange and heavy) are only present in the valence quark sector. For a theoretical treatment of this approximation, see Ref. [3].

sector provides a cross-check of the reliability of our results in the continuum limit.

The continuum operators of interest are expressed, in terms of their lattice counterparts, as follows:

$$V_\mu^{\rm cont} = Z_A A_\mu^{\rm tm} + \mathcal{O}(a^2) = Z_V V_\mu^{\rm OS} + \mathcal{O}(a^2), \qquad (1.5)$$

$$T_{\mu\nu}^{\rm cont} = Z_T T_{\mu\nu}^{\rm tm} + \mathcal{O}(a^2) = Z_T \tilde{T}_{\mu\nu}^{\rm OS} + \mathcal{O}(a^2), \qquad (1.6)$$

where $\tilde{T}_{\mu\nu} = \epsilon_{\mu\nu\rho\sigma} T_{\rho\sigma}$. The vector and axial currents are normalized by the scale independent factors Z_V and Z_A, while $Z_T \equiv Z_T(\mu)$ runs with a renormalization scale μ (i.e. it is defined in a given renormalization scheme).

The vector boson mass, m_V, as well as f_V and f_T, are obtained form two-point correlation functions at zero spatial momenta and large time separations. These are defined in the continuum (Euclidean space-time) as

$$C_V^{\rm cont}(x^0) \equiv \frac{1}{3} \sum_j \int d^3x \langle V_j(x) V_j^\dagger(0) \rangle^{\rm cont}$$
$$\to \frac{f_V^2 m_V}{2} \exp[-m_V T/2] \cosh[m_V(T/2 - x^0)], \qquad (1.7)$$

$$C_T^{\rm cont}(x^0) \equiv \frac{1}{3} \sum_j \int d^3x \langle T_{0j}(x) T_{0j}^\dagger(0) \rangle^{\rm cont}$$
$$\to \frac{f_T^2 m_V}{2} \exp[-m_V T/2] \cosh[m_V(T/2 - x^0)]. \qquad (1.8)$$

The asymptotic expressions of the above equations correspond to the large time limit of the correlation functions (symmetrized in time), with periodic boundary conditions for the gauge fields and (anti)periodic ones for the fermion fields in the (time)space directions (i.e. $0 \ll x^0 \ll T/2$). These are actually the boundary conditions of our lattice simulations. The lattice correlation functions are related to the continuum ones as suggested by Eqs. (1.5) and (1.6):

$$C_V^{\rm cont}(x^0) = Z_A^2 C_A^{\rm tm}(x^0) + \mathcal{O}(a^2) = Z_V^2 C_V^{\rm OS}(x^0) + \mathcal{O}(a^2), \qquad (1.9)$$

$$C_{\tilde{T}}^{\rm cont}(x^0) = Z_T^2 C_T^{\rm tm}(x^0) + \mathcal{O}(a^2) = Z_T^2 C_{\tilde{T}}^{\rm OS}(x_0) + \mathcal{O}(a^2). \qquad (1.10)$$

The meaning of the notation $C_A^{\rm tm}$, $C_{\tilde{T}}^{\rm OS}$, etc. should be transparent to the reader. The ratio f_T/f_V is computed from the square root of the ratio of correlation functions $C_T^{\rm cont}/C_V^{\rm cont}$, in which many systematic effects cancel. We compute the vector meson mass and decay constant from $C_V^{\rm cont}$ and the ratio f_T/f_V from the ratio of correlation functions $C_T^{\rm cont}/C_V^{\rm cont}$. The tensor coupling f_T is then obtained by multiplying f_T/f_V by f_V.

Note that f_V is a scale independent quantity, while $f_T(\mu)$ depends on the renormalization scale μ, as well as

the renormalization scheme. The scale and scheme dependence of the latter quantity is carried by the renormalization factor $Z_T(\mu)$; we opt for the $\overline{\rm MS}$ scheme and for $\mu = 2$ GeV.

II. RESULTS

ETMC has generated $N_f = 2$ configuration ensembles at four values of the inverse gauge coupling; in this work we make use of only three of them. Light mesons consist of a valence quark doublet, with twisted mass $a\mu_\ell$ equal to that of the sea quarks; $a\mu_\ell = a\mu_{\rm sea}$. Heavy-light mesons consist of a valence quark pair ($a\mu_\ell = a\mu_{\rm sea}$, $a\mu_h$). As already stated, these bare quark mass parameters are chosen so as to have light pseudoscalar mesons ("pions") in the range of $280 \le m_{\rm PS} \le 550$ MeV and heavy-light pseudoscalar mesons ("Kaons") in the range $450 \le m_{\rm PS} \le 650$ MeV. The simulation parameters are gathered in Table I.

Our calibrations are based on earlier collaboration results. The ratio r_0/a, known at each value of the gauge coupling β from Ref. [10], allows us to express our raw dimensionless data (quark masses, meson masses, and decay constants) in units of r_0. Knowledge of the renormalization constant Z_P in the $\overline{\rm MS}$ scheme at 2 GeV (see Ref. [11]) enables us to pass from bare quark masses to renormalized ones (again in r_0 units). Using only data with light valence quarks in the tm setup, we have applied the procedure described in Refs. [1,10] for the determination of the physical continuum light quark mass $\mu_{u/d}^{\overline{\rm MS}}$. From the data concerning light and heavy valence quark masses in the tm setup [10], we determine the physical continuum strange-quark mass $\mu_s^{\overline{\rm MS}}(2$ GeV$)$. These quark mass values are listed in Table II. The Sommer scale we use, based on

TABLE I. Simulation details.

β	$a^{-4}(L^3 \times T)$	$a\mu_\ell = a\mu_{\rm sea}$	$a\mu_h$	$N_{\rm meas}$
3.80	$24^3 \times 48$	0.0080, 0.0110	0.0165, 0.0200	180
($a \sim 0.1$ fm)			0.0250	
3.90	$24^3 \times 48$	0.0040	0.0150, 0.0220	400
			0.0270	
	$24^3 \times 48$	0.0064, 0.0085,	0.0150, 0.0220	200
		0.0100	0.0270	
3.90	$32^3 \times 64$	0.0030, 0.0040	0.0150, 0.0220	270/170
($a \sim 0.085$ fm)			0.0270	
4.05	$32^3 \times 64$	0.0030, 0.0060,	0.0120, 0.0150	200
($a \sim 0.065$ fm)		0.0080	0.0180	

TABLE II. The quark mass values (in the $\overline{\rm MS}$ scheme), used in our analysis; see Ref. [10].

$\mu_{u/d}^{\overline{\rm MS}}(2$ GeV$)$	$\mu_s^{\overline{\rm MS}}(2$ GeV$)$
3.6(2) MeV	95(6) MeV

TABLE III.   The renormalization parameters used in our analysis and the r_0/a values at each gauge coupling. Z_V is obtained from a lattice vector Ward identity, while the other renormalization constants are obtained from the regularization independent scheme in momentum space; for details see Ref. [11].

β	Z_V	Z_A	$Z_T^{\overline{\mathrm{MS}}}(2\ \mathrm{GeV})$	$Z_P^{\overline{\mathrm{MS}}}(2\ \mathrm{GeV})$	r_0/a
3.80	0.5816(02)	0.746(11)	0.733(09)	0.411(12)	4.54(07)
3.90	0.6103(03)	0.746(06)	0.743(05)	0.437(07)	5.35(04)
4.05	0.6451(03)	0.772(06)	0.777(06)	0.477(06)	6.71(04)

an analysis with three values of the lattice spacing, is $r_0 = 0.448(5)$ fm. This updates our previous r_0 computation, derived with two β's, cf. Ref. [1]. In short, the physical values of m_π, m_K and f_π have been used for the calibration of the bare parameters.

We see from Eqs. (1.9) and (1.10) that we need to know the renormalization parameters Z_V, Z_A, and Z_T. These quantities, as well as Z_P, have been computed in Ref. [11], in the regularization independent scheme in momentum space (RI/MOM); Z_P and Z_T are perturbatively converted to $\overline{\mathrm{MS}}$. In the same work a Z_V estimate, obtained from a Ward identity, is also provided. In Table III we gather the most reliable estimates of Ref. [11], which we have used in the present analysis, as well as our estimates of the r_0/a ratio.

As can be seen in Table I, at $\beta = 3.90$ we have performed more extensive simulations, which enable us to check in some detail the quality and stability of the measured physical quantities. We wish to highlight straightaway the two problems we have encountered in these tests, performed for the tm setup: (i) For all sea quark masses, when the valence quark attains its lightest value $a\mu_\ell = 0.0040$, the vector meson effective mass has a poor plateau. The situation already improves at the next quark mass $a\mu_\ell = 0.0064$. Nevertheless, since the signal-to-noise ratio behaves as expected (i.e. it drops like

$\exp[-(m_V - m_{PS})x^0])$ the ρ-meson mass and decay constant can still be extracted (see results presented in Ref. [12]). (ii) A poor quality vector meson effective mass is also seen when $\mu_\ell < \mu_{\mathrm{sea}}$. This problem is absent in the pseudoscalar channel. The above problems are easily avoided in the present work, since the quantities of interest are related to the K^*-meson, consisting of a down and a strange valence quark mass ($\mu_{u/d} < \mu_s$).

In unquenched simulations, depending on the values of quark masses, the resonance decay into a two meson $|K, \pi\rangle$ state may mix with $|K^*\rangle$. The threshold for decay is $E_K + E_\pi$, with $E_{K,\pi} = [m_{K,\pi}^2 + (\frac{2\pi}{L})^2]^{1/2}$ (L is the lattice linear extension). Our simulations are performed above threshold, so that the lowest energy state is $|K^*\rangle$ at zero spatial momentum.

We proceed as follows: at each β value, we compute the necessary observables (vector meson mass m_V, vector decay constant f_V, and the ratio f_T/f_V), for all combinations of $a\mu_\ell = a\mu_{\mathrm{sea}}$ and $a\mu_h$ (with $\mu_\ell < \mu_h$). In this way unitarity holds in the light quark sector, while the heavy valence quark mass, in a partially quenched rationale, spans a range around the physical value μ_s. Examples of the quality of our signal are given in Figs. 1 and 2; the lightest mass is $a\mu_{\mathrm{min}}$ and the heavy mass, corresponding to the physical strange value $a\mu_s$, is obtained by interpolation, as will be explained below.
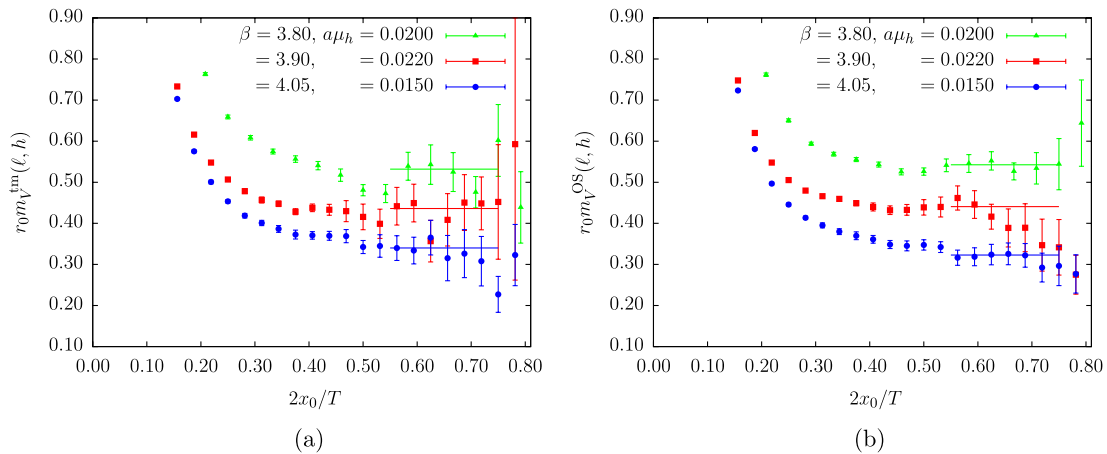

FIG. 1 (color online).   Effective vector meson mass $r_0 m_V$ at three values of the lattice spacing. The light quark mass is $a\mu_{\mathrm{min}}$ (see Table I) and the heavy quark mass $a\mu_h$ is close to that of the physical strange-quark; (a) tm setup, (b) OS setup. Plateau intervals are indicated by straight lines.
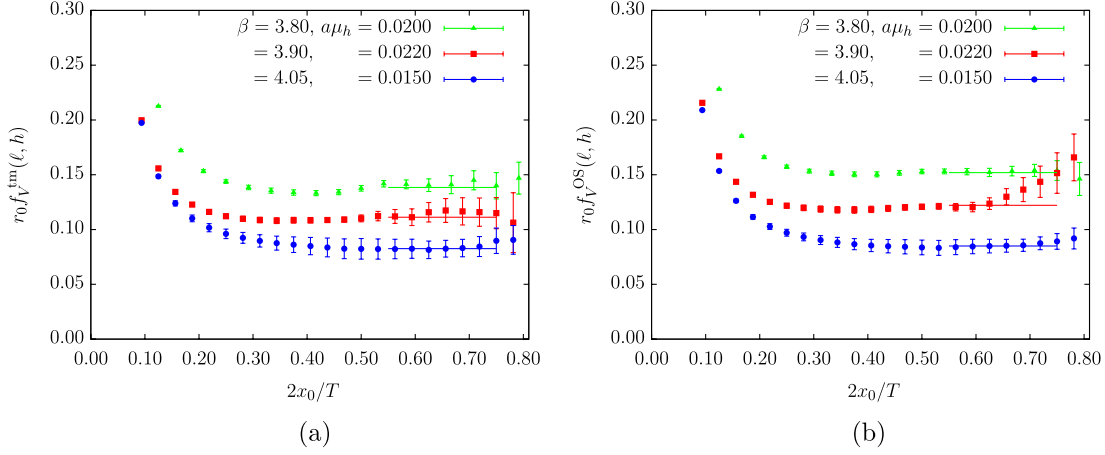
FIG. 2 (color online).   Vector decay constant $r_0 f_V$ at three values of the lattice spacing. The light quark mass is $a\mu_{\min}$ (see Table I) and the heavy quark mass $a\mu_h$ is close to that of the physical strange quark;(a) tm setup, (b) OS setup. Plateaux intervals are indicated by straight lines.
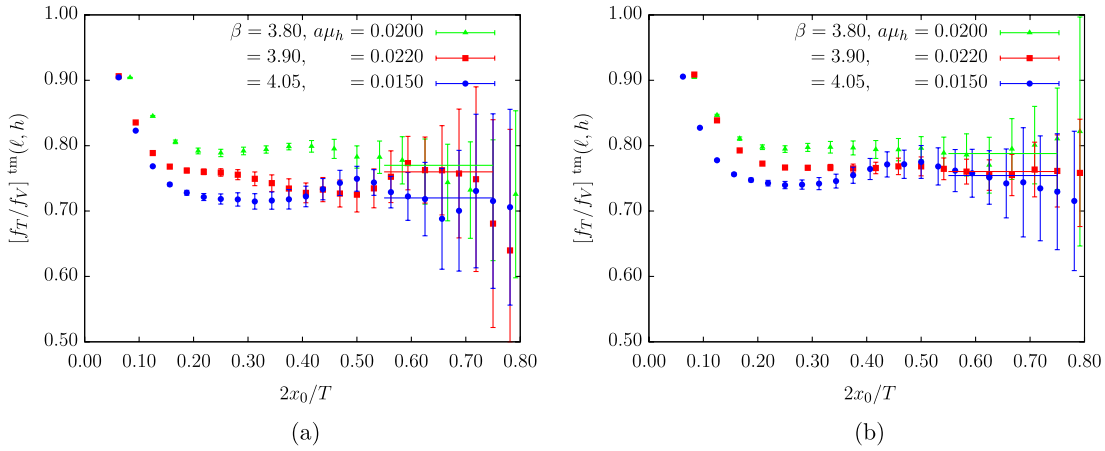

FIG. 3 (color online).   The ratio f_T/f_V in the tm setup, at three values of the lattice spacing and heavy quark mass $a\mu_h$, close to that of the physical strange quark. (a) For the lightest quark mass $a\mu_{\min}$; (b) for the next-to-lightest quark mass. Plateaux intervals are indicated by straight lines.

Statistical errors are estimated with the bootstrap method, employing 1000 bootstrap samples. A reliable direct determination of the ratio f_T/f_V in the OS setup is not possible, because the ratio of correlation functions $C_{\tilde{T}}^{OS}/C_V^{OS}$ do not display satisfactory plateaus, due to big statistical fluctuations of the tensor correlator $C_{\tilde{T}}^{OS}$. We only present f_T/f_V results in the tm setup, obtained from the better behaved correlation function C_T^{tm}. In Fig. 3 we show results for this ratio at $a\mu_{\min}$ and also at a heavier light quark mass.

Regarding vector meson masses m_V and couplings f_V, both tm and OS results display a similar plateau quality and statistical accuracy. At finite lattice spacing and for equal bare quark masses, tm and OS estimates of m_V are compatible within errors. Agreement is also very good for f_V, with occasional discrepancies, interpreted as cutoff effects,

showing up at the coarsest lattice.[2] Contrary to the well-known large $\mathcal{O}(a^2)$ isospin breaking effects in the neutral to charged pion splitting mass, no numerically large differences are observed between tm and OS results for f_V and m_V. This fact is in agreement with theoretical expectations, see Ref. [13].

The extrapolation to the physical quark masses is carried out in two steps. First, for fixed values of the gauge coupling β and light quark mass $a\mu_\ell = a\mu_{sea}$, we perform linear interpolations of $r_0 m_V$, $r_0 f_V$, and f_T/f_V to the physical strange-quark mass μ_s. The second step consists in using these interpolated results for a combined fit of our

_____

[2]Given the large fluctuations of f_T/f_V in the OS setup at the finer lattice spacing, we only quote results for this ratio in the tm-setup.

TABLE IV.   Results for three values of lattice spacing and several light quark masses $a\mu_\ell$, interpolated to the physical strange mass μ_s. Vector mass and vector decay constant results are presented for both tm and OS setups. The ratio f_T/f_V results are given only in the tm setup. Our extrapolations at the $\mu_{u/d}$ physical point and in the continuum limit are also shown. In the last row the experimental results for the vector mass and the vector decay constant, in units of r_0, have been added.

β	$a\mu_l$	$r_0 m_V^{\rm tm}(\ell, s)$	$r_0 m_V^{\rm OS}(\ell, s)$	$r_0 f_V^{\rm tm}(\ell, s)$	$r_0 f_V^{\rm OS}(\ell, s)$	$[f_T/f_V]^{\rm tm}(\ell, s)$
3.80	0.0080	2.443(41)	2.471(30)	0.642(18)	0.700(13)	0.764(38)
	0.0110	2.508(32)	2.500(23)	0.651(14)	0.706(15)	0.792(35)
3.90	0.0040	2.410(41)	2.381(38)	0.610(21)	0.643(17)	0.755(19)
	0.0064	2.441(32)	2.427(35)	0.626(22)	0.659(12)	0.726(20)
	0.0085	2.484(48)	2.441(33)	0.628(16)	0.652(16)	0.776(27)
	0.0100	2.468(54)	2.481(32)	0.619(20)	0.657(16)	0.774(31)
	0.0030($L = 32$)	2.259(75)	2.335(45)	0.577(20)	0.639(16)	0.714(20)
	0.0040($L = 32$)	2.364(32)	2.371(50)	0.599(22)	0.640(21)	0.722(19)
4.05	0.0030	2.305(86)	2.263(80)	0.568(49)	0.588(40)	0.742(27)
	0.0060	2.439(67)	2.295(76)	0.618(41)	0.578(46)	0.768(30)
	0.0080	2.512(65)	2.427(48)	0.649(31)	0.648(27)	0.741(31)
CL	$\mu_{u/d}$	2.227(71)	2.200(60)	0.545(41)	0.525(30)	0.701(46)
expt.		2.025		0.493		

data at three lattice spacings and all available light quark masses, in order to determine the continuum value of the quantity of interest ($r_0 m_V$, $r_0 f_V$, and f_T/f_V; see Figs. 4–6, respectively). We model our data with the following *ansatz*:

$$m_V r_0 = C_0(\mu_s r_0) + C_1(\mu_s r_0)\mu_\ell r_0 + D(\mu_s r_0)\frac{a^2}{r_0^2}, \quad (2.1)$$

and similarly for $f_V r_0$ and f_T/f_V.

The results of the interpolations in the heavy quark mass μ_h to the physical value μ_s, at each β and $a\mu_\ell$, are gathered in Table IV. Errors are due to (i) statistical fluctuations, (ii) the uncertainty of the strange-quark mass μ_s when interpolating in μ_h, (iii) the uncertainty of r_0/a, and

(iv) the errors of renormalization constants Z_A and Z_T (where applicable).

In the same table we also display the results of the combined chiral and continuum extrapolations. The uncertainty of these estimates includes, besides the fitting error, also that of $\mu_{u/d}$. As previously stated, the whole error analysis is based on the bootstrap method. Note that for the three quantities of interest, m_V, f_V and f_T/f_V, the value of $\chi^2/$d.o.f. is less than unity. The linear dependence of our data on the light quark mass agrees with the predictions of chiral perturbation theory (extended by the inclusion of tensor external sources) for the ratio f_T/f_V in the K^* mass range; see Refs. [14,15].

Our final results, extracted in the tm setup, are

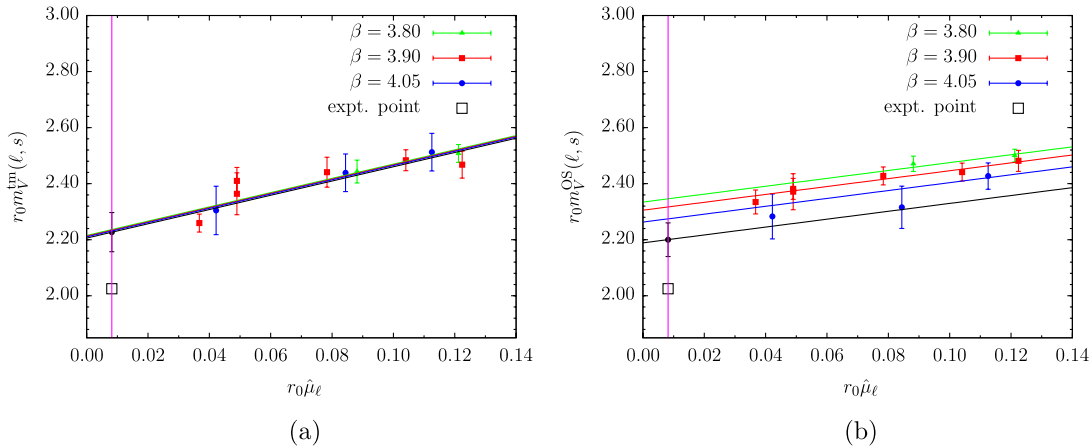$$m_{K^*} = 981(31)(10)[33] \text{ MeV}, \quad (2,2)$$

FIG. 4 (color online). $r_0 m_V$ plotted against the renormalized light quark mass $r_0\hat{\mu}_\ell$; (a) tm setup, (b) OS setup. The continuous lines are combined chiral and continuum extrapolations to the physical point. The bottom (black) line corresponds to Eq. (2.1) at $a = 0$. The separation among the four lines in (a) is invisible to the naked eye (i.e. small scaling violations).
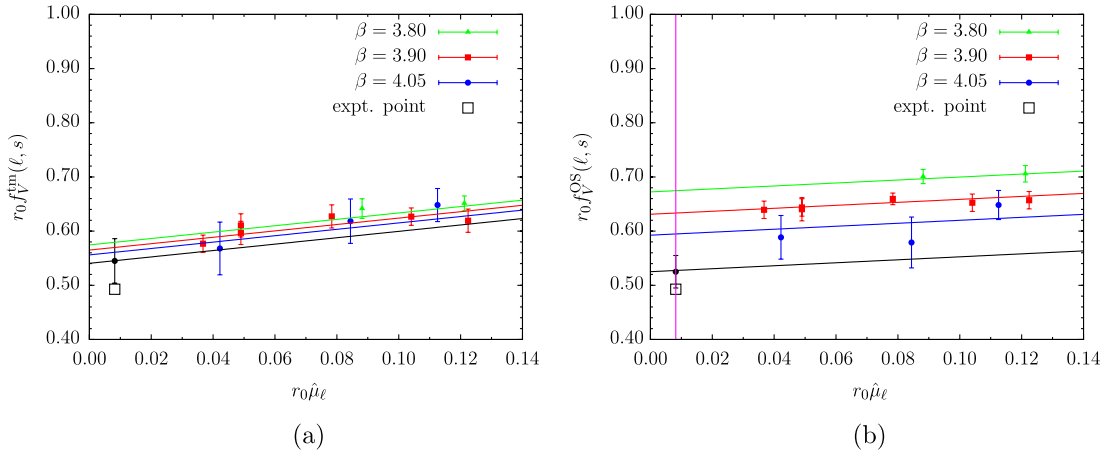
FIG. 5 (color online). $r_0 f_V$ plotted against the renormalized light quark mass $r_0 \hat{\mu}_\ell$; (a) tm setup, (b) OS setup. The continuous lines are combined chiral and continuum extrapolations to the physical point. The bottom (black) line corresponds to Eq. (2.1) at $a = 0$.
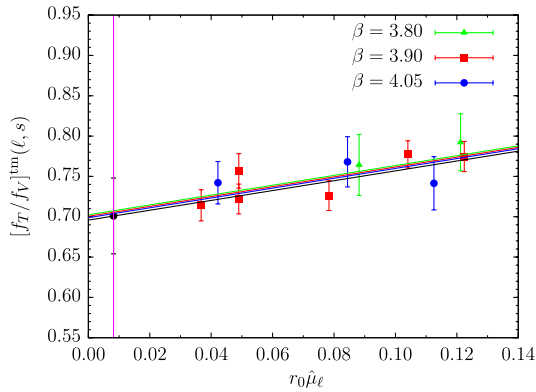

FIG. 6 (color online). f_T/f_V plotted against the renormalized light quark mass $r_0 \hat{\mu}_\ell$ in the tm setup. The continuous lines are combined chiral and continuum extrapolation to the physical point. The bottom (black) line corresponds to Eq. (2.1) at $a = 0$. The four lines are almost indistinguishable (i.e. small scaling violations).

$$f_{K^*} = 240(18)(02)[18] \text{ MeV}. \qquad (2.3)$$

The first error includes the statistical uncertainty and the systematic effects related to the simultaneous chiral and continuum fits, mass interpolations and extrapolations, and uncertainties in the renormalization parameters. The second error arises from that of r_0. These two errors, combined in quadrature, give the total error in the square brackets. It is encouraging that these results agree with the ones obtained in the OS setup (which is a different regularization), namely, $m_{K^*} = 969(27)(10)[29]$ MeV and $f_{K^*} = 231(13)(02)[13]$ MeV. Compared to the experimentally known values, $m_{K^*} = 892$ MeV and $f_{K^*} = 217$ MeV, the vector meson mass is 2–3 standard deviations off, while the decay constant is compatible within

about 1 standard deviation. The overestimation of m_{K^*} is presumably due to the fitting ansatz, which does not take resonance effects into account. A more sophisticated treatment of the extrapolation, or a lattice study nearer the physical point could address these issues along the lines of Ref. [12]. This is beyond the scope of the present work.

Our final estimate (tm setup) for the ratio of vector meson couplings is

$$\left. \frac{f_T(2 \text{ GeV})}{f_V} \right|_{K^*} = 0.704(41). \qquad (2.4)$$

This is compatible with the continuum limit quenched result $[f_T(2 \text{ GeV})/f_V]_{K^*} = 0.739(17)(3)$ of Ref. [16]. We are also in agreement with the result of the RBC/UKQCD Collaboration [17]; using $N_f = 2 + 1$ dynamical fermions at a single lattice spacing, they quote $[f_T(2 \text{ GeV})/f_V]_{K^*} = 0.712(12)$. The lattice results are also in agreement with the sum rules' estimate $[f_T(2 \text{ GeV})/f_V]_{K^*} = 0.73(4)$, quoted in [18].

Nevertheless, the difference between the physical vector mass m_{K^*} and our result (2,2) indicates that it is essential to perform simulations in the vicinity of the physical point, in order to make reliable predictions.

[1] R. Baron *et al.* (ETM Collaboration), J. High Energy Phys. 08 (2010) 097.

[2] R. Frezzotti *et al.*, J. High Energy Phys. 08 (2001) 058.

[3] C. W. Bernard and M. F. Golterman, Phys. Rev. D **46**, 853 (1992).

[4] K. Osterwalder and E. Seiler, Ann. Phys. (N.Y.) **110**, 440 (1978).

[5] C. Pena, S. Sint, and A. Vladikas (ALPHA Collaboration), J. High Energy Phys. 09 (2004) 069.

[6] R. Frezzotti and G. C. Rossi, J. High Energy Phys. 10 (2004) 070.

[7] R. Frezzotti and G. C. Rossi, J. High Energy Phys. 08 (2004) 007.

[8] P. Dimopoulos *et al.* (ALPHA Collaboration), Nucl. Phys. **B776**, 258 (2007).

[9] P. Dimopoulos, H. Simma, and A. Vladikas, J. High Energy Phys. 07 (2009) 007.

[10] B. Blossier *et al.* (ETM Collaboration), Phys. Rev. D **82**, 114513 (2010).

[11] M. Constantinou *et al.* (ETM Collaboration), J. High Energy Phys. 08 (2010) 068.

[12] K. Jansen *et al.* (ETM Collaboration), Phys. Rev. D **80**, 054510 (2009).

[13] P. Dimopoulos, R. Frezzotti, C. Michael, G. Rossi, and C. Urbach, Phys. Rev. D **81**, 034509 (2010).

[14] O. Cata and V. Mateu, J. High Energy Phys. 09 (2007) 078.

[15] O. Cata and V. Mateu, Nucl. Phys. **B831**, 204 (2010).

[16] D. Becirevic *et al.*, J. High Energy Phys. 05 (2003) 007.

[17] C. Allton *et al.* (RBC-UKQCD Collaboration), Phys. Rev. D **78**, 114509 (2008).

[18] P. Ball, G. W. Jones, and R. Zwicky, Phys. Rev. D **75**, 054004 (2007).